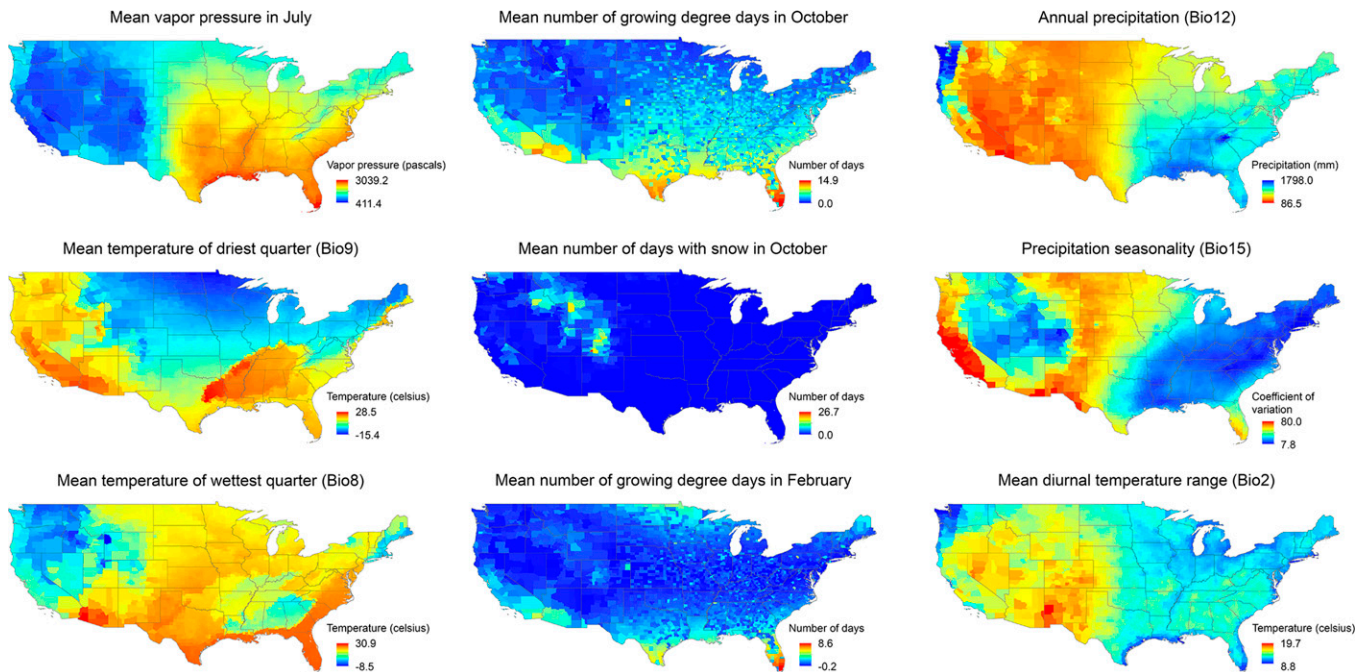


SUPPLEMENTAL MATERIAL

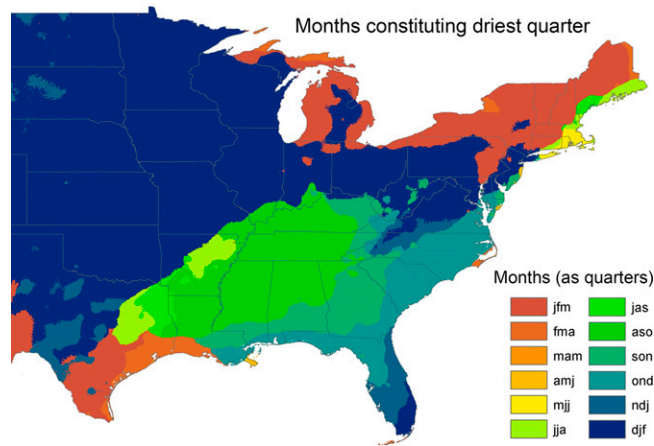
**Supplemental material 1.** Calculation of GDD predictor values was complicated by the fact that while GDDs are typically derived using daily temperature data, the data available through WorldClim have a monthly resolution. To determine whether GDDs calculated using monthly data could accurately approximate true GDDs (i.e., derived from daily data), and to quantify a mathematical relationship with which the former could be converted to the latter, we obtained 34 years (1980–2013) of daily meteorological records from Daymet<sup>62</sup> for 15 representative cities distributed across the current distribution of *Amblyomma americanum* according to Springer and others.<sup>56</sup> Using these data, and a biologically based threshold value of 10°C,<sup>63</sup> we calculated true GDDs using daily data  $[(\text{GDD}_d = (\text{daily } T_{\text{max}} + \text{daily } T_{\text{min}})/2 - 10)]$ , with negative values set to zero) and approximate GDDs using monthly data  $[(\text{GDD}_m = (\text{average of monthly } T_{\text{max}} + \text{average of monthly } T_{\text{min}})/2 - 10)]$ . For each city,  $\text{GDD}_d$  values were averaged for each month within each year, and then both  $\text{GDD}_d$  and  $\text{GDD}_m$  values were averaged for each month across all years. Using the resulting 180 pairs of monthly averaged values (15 cities  $\times$  12 months, denoted  $\text{mGDD}_d$  and  $\text{mGDD}_m$ ) we found that the former could be predicted almost exactly using the latter with the robust quadratic relationship  $\text{mGDD}_d = 1.95 + (0.69 \times \text{mGDD}_m) + \{0.023 \times [(\text{mGDD}_m - 4.41)^2]\}$  ( $r_{\text{adj}}^2 = 0.9974$ , mean square statistic [MS] = 3,258.7,  $F_{2,179} = 34,335.3$ ,  $P < 0.0001$ ). We applied this equation to calculate GDDs using the monthly temperature data avail-

able in WorldClim. For each climate data grid cell we calculated  $\text{mGDD}_d$  for each month alone (e.g., for April,  $\text{mGDD}_d(\text{APR})$  calculated with the quadric relationship where  $\text{mGDD}_m(\text{APR}) = \{[(\text{average April } T_{\text{max}} + \text{average April } T_{\text{min}})/2] - 10\}$  using average maximum and minimum temperatures in April 1950–2000) and for each month cumulative from the start of the year (e.g., for April,  $\text{mGDD}_d(\text{APR-CUM})$  calculated as  $\text{mGDD}_d(\text{JAN}) + \text{mGDD}_d(\text{FEB}) + \text{mGDD}_d(\text{MAR}) + \text{mGDD}_d(\text{APR})$ ). GDD = growing degree day

**Supplemental material 2.** To calculate mean vapor pressure in July using historical values of vapor pressure (from Daymet) and mean temperature (from WorldClim), we first calculated the historical saturation vapor pressure in July as a function of historical mean temperature in July  $\{[\text{Historical saturation vapor pressure}_{\text{July}} = 611 \times 10^{(7.5 \times \text{Historical mean monthly temperature}_{\text{July}})/(237.3 + \text{Historical mean monthly temperature}_{\text{July}})]\}$ . Second, we calculated the historical relative humidity in July as the ratio of the historical vapor pressure in July and the historical saturation vapor pressure in July  $[\text{Historical relative humidity}_{\text{July}} = 100 \times (\text{Historical vapor pressure}_{\text{July}}/\text{Historical saturation vapor pressure}_{\text{July}})]$ . Third, we used the formula provided in the first step to calculate future saturation vapor pressure in July as a function of future mean temperature in July. Finally, we rearranged the formula used in the second step to calculate future vapor pressure in July as a function of historical relative humidity in July and future saturation vapor pressure in July  $[\text{Future vapor pressure}_{\text{July}} = (\text{Historical relative humidity}_{\text{July}} \times \text{Future saturation vapor pressure}_{\text{July}})/100]$ .

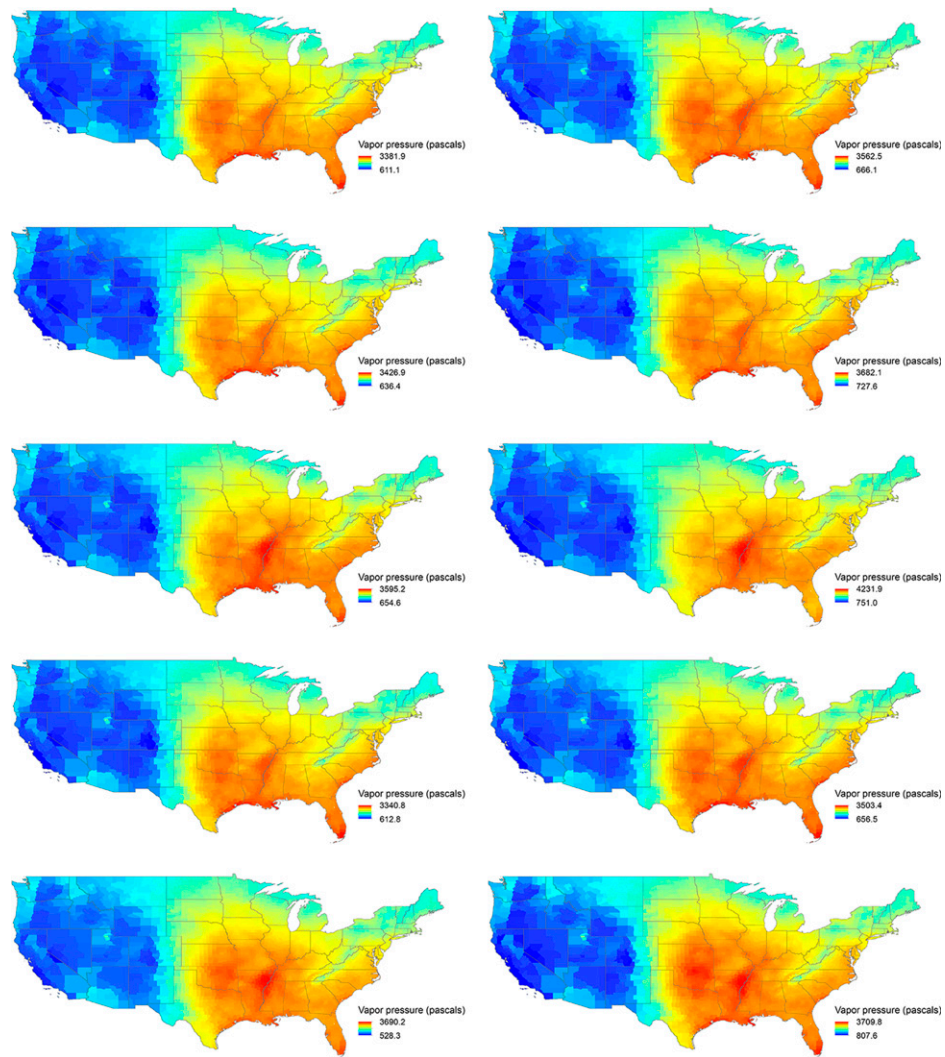


SUPPLEMENTAL FIGURE 1. Maps showing values of the nine climate predictor variables used in the present-day distribution modeling.



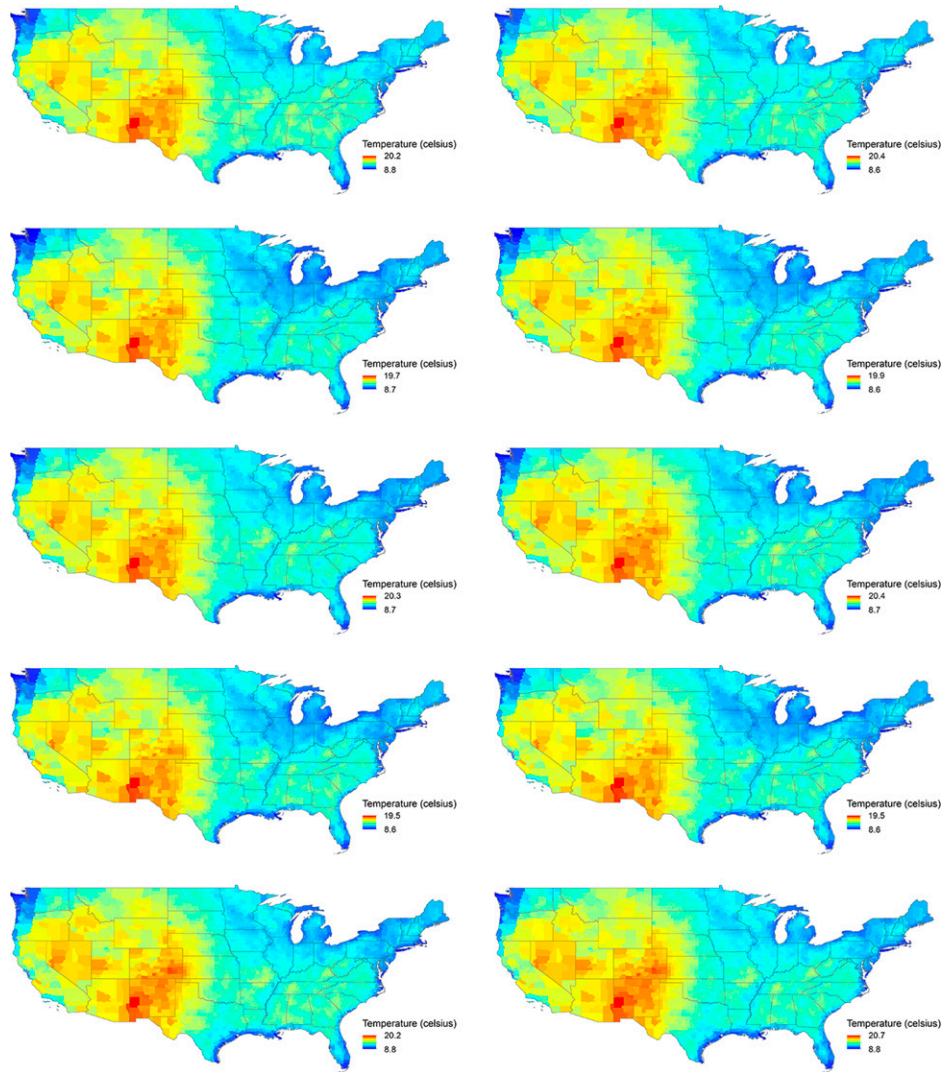
SUPPLEMENTAL FIGURE 2. Map showing geographic variation in the timing of the driest quarter within central and eastern portions of the continental United States. All possible quarters (combinations of three consecutive months) are shown.

### Future vapor pressure in July



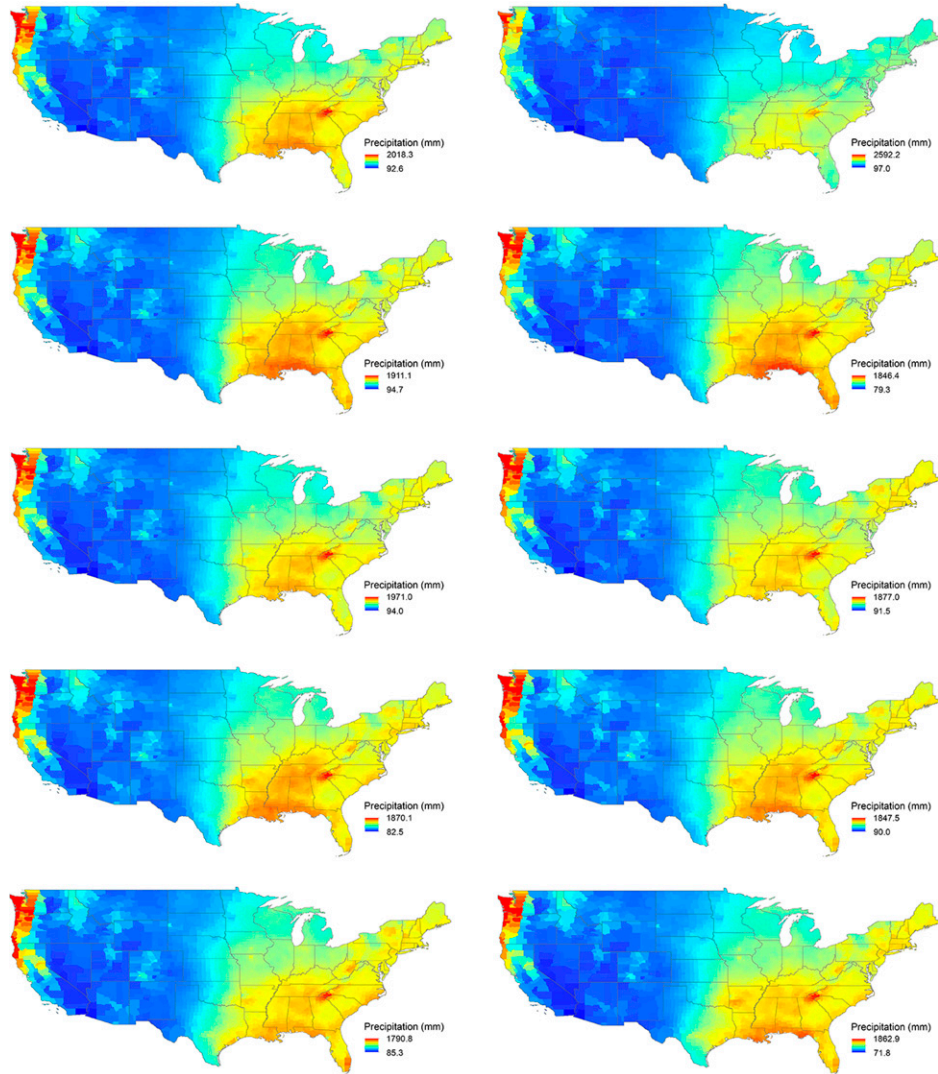
SUPPLEMENTAL FIGURE 3. Maps showing predicted future values of mean vapor pressure in July generated by each unique combination of Atmosphere Ocean General Circulation Model (AOGCM,  $N = 5$ ) and Representative Concentration Pathway (RCP) emissions scenario ( $N = 2$ ). AOGCMs by rows (top to bottom) are version 4 of the Community Climate System Model, the low-resolution version of the Max Planck Institute Earth System Model, the full-earth-system version of the Met Office Hadley Center second generation family of coupled climate models, CNRM-CM5, and ACCESS1-0. In each row, results associated with the RCP4.5 emissions scenario are on the left, those associated with the RCP8.5 scenario are on the right.

### Future mean diurnal temperature range (Bio2)



SUPPLEMENTAL FIGURE 4. Maps showing predicted future values of mean diurnal temperature range (Bio2) generated by each unique combination of Atmosphere Ocean General Circulation Model (AOGCM,  $N = 5$ ) and Representative Concentration Pathway (RCP) emissions scenario ( $N = 2$ ). AOGCMs by rows (top to bottom) are version 4 of the Community Climate System Model, the low-resolution version of the Max Planck Institute Earth System Model, the full-earth-system version of the Met Office Hadley Center second generation family of coupled climate models, CNRM-CM5, and ACCESS1-0. In each row, results associated with the RCP4.5 emissions scenario are on the left, those associated with the RCP8.5 scenario are on the right.

## Future annual precipitation (Bio12)



SUPPLEMENTAL FIGURE 5. Maps showing predicted future values of annual precipitation (Bio12) generated by each unique combination of Atmosphere Ocean General Circulation Model (AOGCM,  $N = 5$ ) and Representative Concentration Pathway (RCP) emissions scenario ( $N = 2$ ). AOGCMs by rows (top to bottom) are version 4 of the Community Climate System Model, the low-resolution version of the Max Planck Institute Earth System Model, the full-earth-system version of the Met Office Hadley Center second generation family of coupled climate models, CNRM-CM5, and ACCESS1-0. In each row, results associated with the RCP4.5 emissions scenario are on the left, those associated with the RCP8.5 scenario are on the right.

SUPPLEMENTAL TABLE 1

For every county within each of the continental United States, unique Federal Information Processing Standard (FIPS) code and associated classification of *Amblyomma americanum* collection records or predictions about the distribution of suitable habitat. County-level classification of *A. americanum* collection records, cumulative from 1898 through 2012 (established, reported, no records), based on results in Springer and others.<sup>56</sup> Two counties that could have been classified as “established” based on collection records, but that were categorized as background (presumed absence) locations in our analyses, are indicated with an asterisk (Sacramento county, California and Ravalli county, Montana). For present-day distribution modeling, habitat suitability scores are provided for each of the five optimized models. Consensus habitat suitability scores are provided for the present-day ensemble model, the RCP4.5 future ensemble prediction, and the RCP8.5 future ensemble prediction. Consensus MESS scores are provided for the two future ensemble predictions